UvA-DARE (Digital Academic Repository)

Ferromagnetism, superconductivity and quantum criticality in uranium intermetallics

Nguyen Thanh, H.

Publication date
2008

Citation for published version (APA):
Nguyen Thanh, H. (2008). *Ferromagnetism, superconductivity and quantum criticality in uranium intermetallics*. [Thesis, fully internal, Universiteit van Amsterdam].

6. Evolution of magnetism in URhGe doped with Si and Co

6.1. Introduction

In the search for a FM QCP in URhGe, chemical substitution offers a promising route. For doping on the Rh site, we choose Ru and Co because UCoGe and URuGe are isostructural to URhGe and both are reported to have a paramagnetic ground state [39,115,151]. As reported in Chapter 4, measurements of the magnetization, resistivity, specific heat and ac-susceptibility provide evidence for a continuous FM QPT by replacing Rh with Ru at the critical concentration of Ru $x_{cr} = 0.38$. It is therefore expected that substitution of Rh by Co will also reduce the Curie temperature and lead to the approach of the magnetic instability.

Among the URhX compounds where X is a nearest neighboring element of Ge, only URhSi is isostructural to URhGe. Since URhSi is a ferromagnet with a Curie temperature of 9.5 K [39,115,117], we do not expect one can tune URhGe to a QCP by Si doping. Nevertheless, it is meaningful to study the evolution of magnetism in URhGe by Si doping. Notice that Co and Rh, and Si and Ge, are isoeletronic. Therefore we expect that the hybridization phenomena leading to magnetic order are controlled to first order by the volume effect when alloying with Co and Si (the unit cell volume of UCoGe and URhSi are both smaller than the one of URhGe). In the case of Ru doping, the hybridization is influenced by both the volume effect (the unit cell volume of URuGe is smaller than the one of URhGe) and the effect of depletion of the d-band (Ru has one electron less than Rh).

In this chapter, we report the evolution of ferromagnetic order in the URhGe$_{1-x}$Si$_x$ and URh$_{1-x}$Co$_x$Ge series via a study of the magnetic and transport properties on polycrystalline samples. For Si doping, the data reveal no significant change of the ferromagnetic

properties. T_C is constant for a Si concentration up to $x = 0.20$ and exhibits a small increase to a value of 10.5 K for $x = 1$. For Co doping, T_C first increases up to 20 K for $x = 0.60$, beyond which T_C drops to 3 K for $x = 1$. Thus we find that the end compound UCoGe has a ferromagnetic rather than a paramagnetic ground state, as was reported previously in Refs.[39,115,151]. Moreover, ferromagnetism coexists with superconductivity in UCoGe, as will be described in Chapter 7.

6.2. URhGe$_{1-x}$Si$_x$

6.2.1. Sample preparation and characterization

Polycrystalline URhGe$_{1-x}$Si$_x$ samples with $x = 0$, 0.1, 0.2 and 1, were prepared under the same conditions as the URh$_{1-x}$Ru$_x$Ge alloys. The constituents U, Rh (3N purity) and Ge, Si (5N purity) were melted together in the arc-furnace under a high-purity argon atmosphere. The weight loss was less than 0.1 %. The as-cast buttons were annealed for 10 days at 875 ^{o}C. The magnetization and transport properties were investigated on bar-shape samples cut by spark erosion.

The lattice parameters for the URhGe$_{1-x}$Si$_x$ alloys ($x = 0.1$, 0.2 and 1.0) have not been determined. However, given the literature values for URhSi ($a = 7.024$ Å, $b = 4.121$ Å and $c = 7.458$ Å) [152] and assuming Vegard's law [124], we conclude that the a parameter expands and the b and c parameters contract with increasing Si content. The unit cell volume decreases linearly at a rate of 0.084 Å^3/at.% Si to $\Omega = 215.9$ Å^3 for URhSi [152].

6.2.2. Magnetization

In Fig. 6.1, the magnetization $M(T)$ measured in 0.01 T and its derivative d$M(T)$/dT for the URhGe$_{1-x}$Si$_x$ series, with $x = 0.0$, 0.10, 0.20 and 1.0, is shown as a function of temperature. Ferromagnetic order is robust in the case of Si doping. The Curie temperatures deduced from (d$M(T)$/dT)$_{min}$ agree with those deduced from the Arrott plots (not shown), as expected. T_C does not change with Si content up to $x = 0.20$. For the end compound URhSi we find $T_C = 10.4$ K. This value is slightly higher than T_C given in the literature for polycrystalline samples [39,115,117] but coincides with T_C obtained on a single crystal [153]. In Ref.[153] the higher T_C of the single crystal was tentatively attributed to Si deficiency. The $M(T)$ curves in Fig. 6.1 are well described by Eq. 4.2 with the spin-
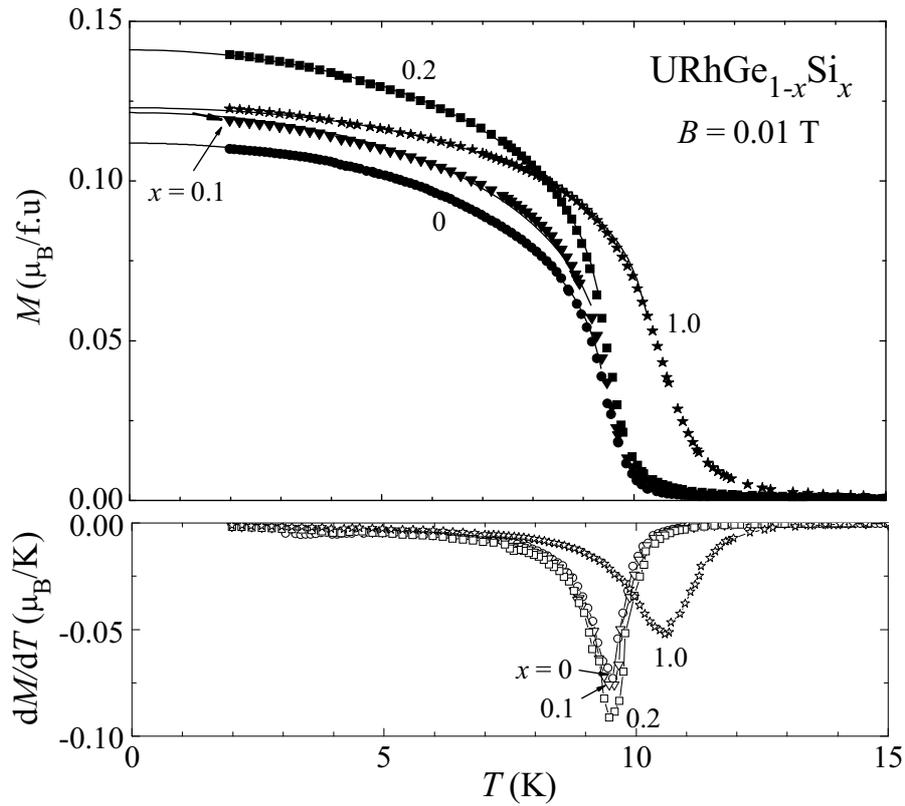
Figure 6.1 Upper frame: Temperature variation of the dc-magnetization measured in a field B = 0.01 T of URhGe$_{1-x}$Si$_x$ alloys. The solid lines present fits to Eq. 4.1. *Lower frame*: Temperature derivative of the magnetization.

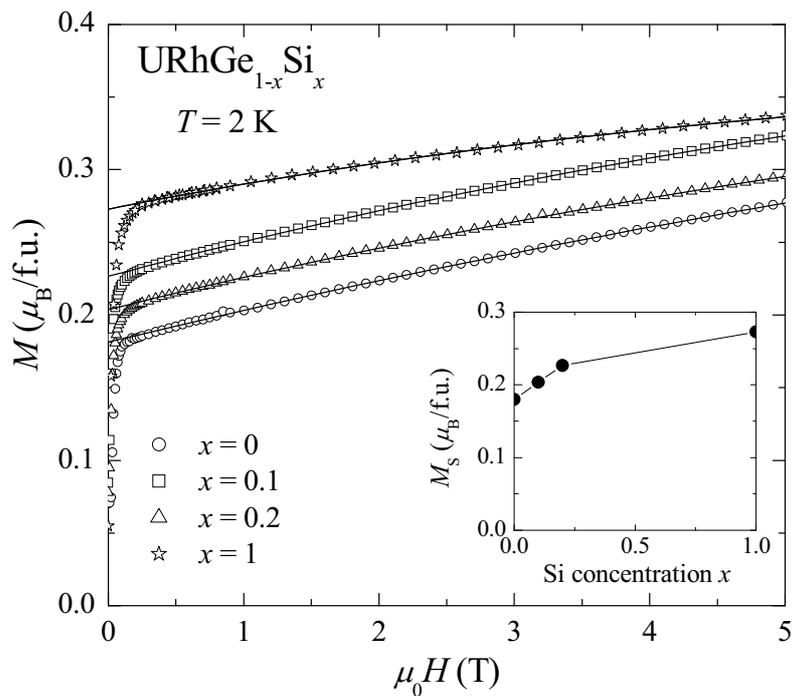*Figure 6.2 M(B)* curves of URhGe$_{1-x}$Si$_x$ measured in a field up to 5 T at 2 K. The solid lines represent fits to Eq. 4.3. *Inset*: M_S of URhGe$_{1-x}$Si$_x$ as a function of Ru concentration.
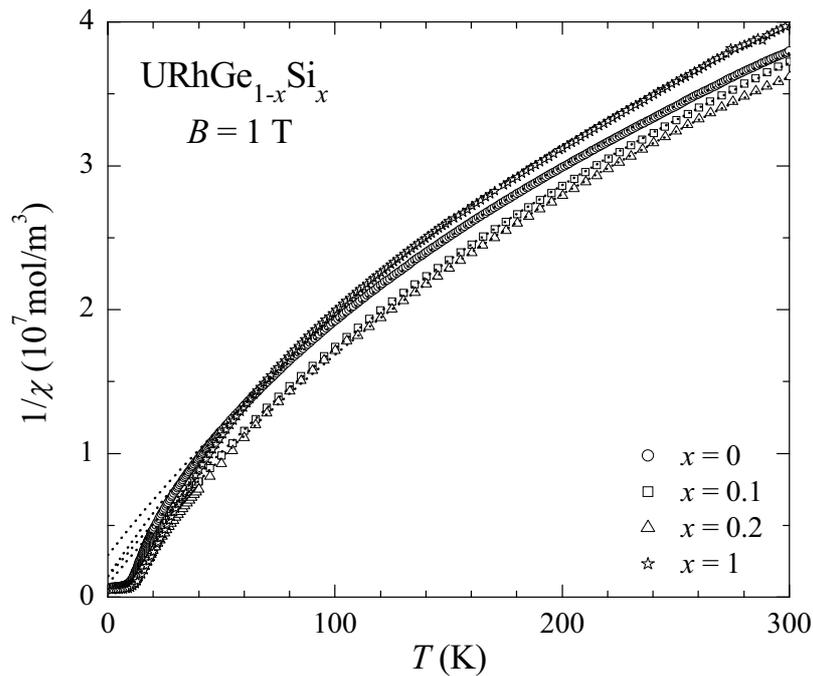
Figure 6.3 Temperature variation of the reciprocal susceptibility of URhGe$_{1-x}$Si$_x$ alloys measured in a field of 1 T. The dotted lines are the best fits to the MCW law in the temperature range $T = 50$ - 300 K.

Table 6.1 The Curie temperature T_C, the spontaneous moment M_S, the effective moment p_{eff} and the paramagnetic Curie temperature θ of URhGe$_{1-x}$Si$_x$ alloys as deduced from magnetization measurements.

x-Si	T_C (K)	M_S (μ_B/f.u.)	p_{eff} (μ_B/f.u.)	θ (K)
0	9.6	0.18	1.72	-14.1
0.1	9.6	0.20	1.80	-7.9
0.2	9.5	0.23	1.79	-4.6
1	10.4	0.27	1.64	-6.2

wave exponent fixed at $\alpha = 2$ and the critical exponent $\beta = 0.20$ - 0.35, which compares well with the theoretical value $\beta = 0.325$ for 3D Ising-like ferromagnets [127,128].

The magnetization measured in an applied field up to 5 T at 2 K is shown in Fig. 6.2. The spontaneous magnetic moment M_S, which is extrapolated from higher fields towards zero field (following Eq. 4.3), slightly increases upon Si doping, as shown in the inset of Fig. 6.2. For pure URhSi, $M_S = 0.27$ μ_B/f.u. in good agreement with the value derived from the magnetization measurements previously reported in the literature [116,117].

The reciprocal susceptibility, $1/\chi$, of URhGe$_{1-x}$Si$_x$ measured in a field $B = 1$ T in the

temperature range 2 - 300 K is plotted in Fig. 6.3. The data show only a weak variation with Si content. In the temperature range 50 - 300 K, the susceptibility can be well described by the MCW law resulting in a temperature independent susceptibility $\chi_0 \sim 10^{-8}$ m^3/mol. The effective moment p_{eff} and the paramagnetic Curie temperature θ of URhGe$_{1-x}$Si$_x$ obtained by fitting $\chi(T)$ to Eq. 4.2 are listed in Table 6.1.
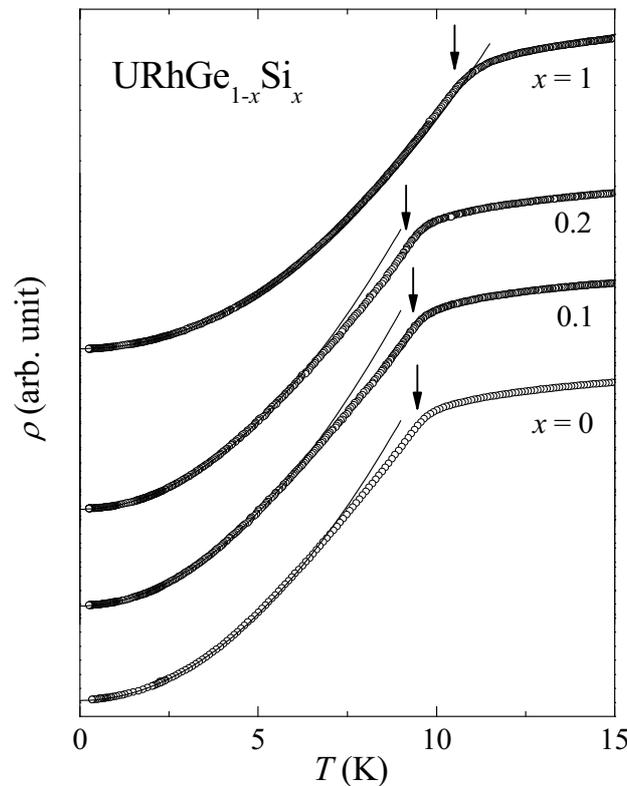
6.2.3. Electrical resistivity

Figure 6.4 Temperature variation of the electrical resistivity ρ (in arbitrary units) of URhGe$_{1-x}$Si$_x$ alloys with $0 \leq x \leq 1$ for 0.25 K $\leq T \leq$ 15 K. Curie temperatures are indicated by arrows. The solid lines are fits to $\rho = \rho_0 + AT^n$ for $T < 7$ K.

In Fig. 6.4, the electrical resistivity of URhGe$_{1-x}$Si$_x$ alloys as a function of temperature is shown. Note that the vertical scale is in arbitrary units and the curves are shifted for clarity. The $\rho(T)$ curves exhibit the characteristics of ferromagnetic compounds: a nearly temperature independent spin-disorder scattering for $T > T_C$, and for $T < T_C$ scattering at magnons with $\rho \sim T^2$. The Curie temperatures are identified by the maxima in dρ/dT (arrows in Fig. 6.4) in good agreement with the values obtained from magnetization data. The residual resistance ratio *RRR* for URhGe equals 6 and drops to 2 for the Si-doped

samples. However for the end compound URhSi *RRR* = 30 is much larger. The transport parameters are collected in Table 6.2.

Table 6.2 The Curie temperature and the parameters ρ_0, $n = 2$ and *A* obtained by fitting the resistivity to $\rho = \rho_0 + AT^n$ for URhGe$_{1-x}$Si$_x$ alloys.

x-Si	T_C (K)	ρ_0 (µΩcm)	*n*	*A* (µΩcm/K^2)
0	9.4	78	2	6.21
0.1	9.4	209	2	4.24
0.2	9.3	306	2	3.40
1	10.2	14	2	2.00

6.3. URh$_{1-x}$Co$_x$Ge

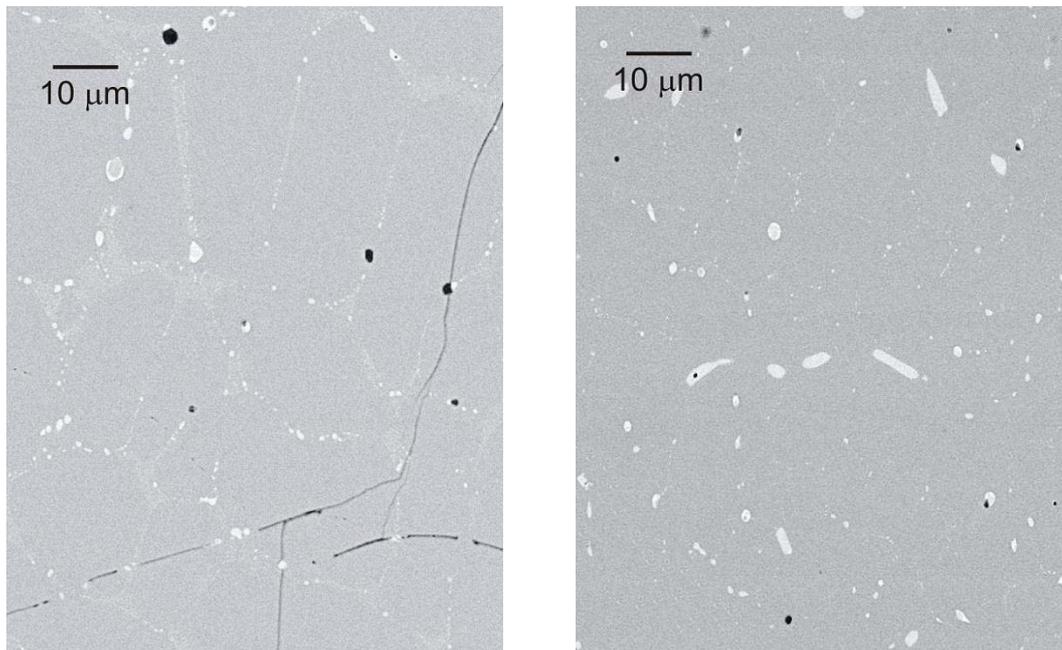### 6.3.1. Sample preparation and characterization

Figure 6.5 EPMA micrographs of URh$_{0.2}$Co$_{0.8}$Ge (*left panel*) and UCoGe (*right panel*). The grey areas represent the main matrix. The (big and small) light spots are the Uranium rich phases. The black spots and black lines are holes and cracks on the surface, respectively.

Polycrystalline URh$_{1-x}$Co$_x$Ge samples, with *x* in the range of $0 \leq x \leq 1$, were prepared by arc-melting the constituents U, Rh, Co (3N purity) and Ge (5N purity) under a high-purity argon atmosphere. The weight loss amounted to ~ 0.03 %. The as-cast buttons were

annealed for 10 days at 875 °C. Bar-shape samples were cut by spark erosion for different experiments (magnetization and transport measurements).

The chemical composition of the samples was checked by EPMA. For all concentrations, the main matrix 1:1:1 comprises about 98% of the samples. Small amounts (2 - 3%) of Uranium rich impurity phases, mainly located at the grain boundaries were detected (see Fig. 6.5) and tiny cracks are observed for the doped samples.

The measured variation of the lattice parameters in the $URh_{1-x}Co_xGe$ series is shown in Fig. 6.6. Here the b and c lattice parameters show a linear decrease, while the a parameter remains almost constant. The unit cell volume decreases linearly at a rate of 0.152 $Å^3$/at.% Co. For UCoGe we obtain a = 6.845 Å, b = 4.206 Å and c = 7.222 Å, with Ω = 207.95 $Å^3$, in good agreement with literature [151]. The shortest U-U distance, d_{U-U}, calculated from the structural parameters, linearly reduces upon Co doping at a rate of -0.52×10^{-3} Å/at.% Co.
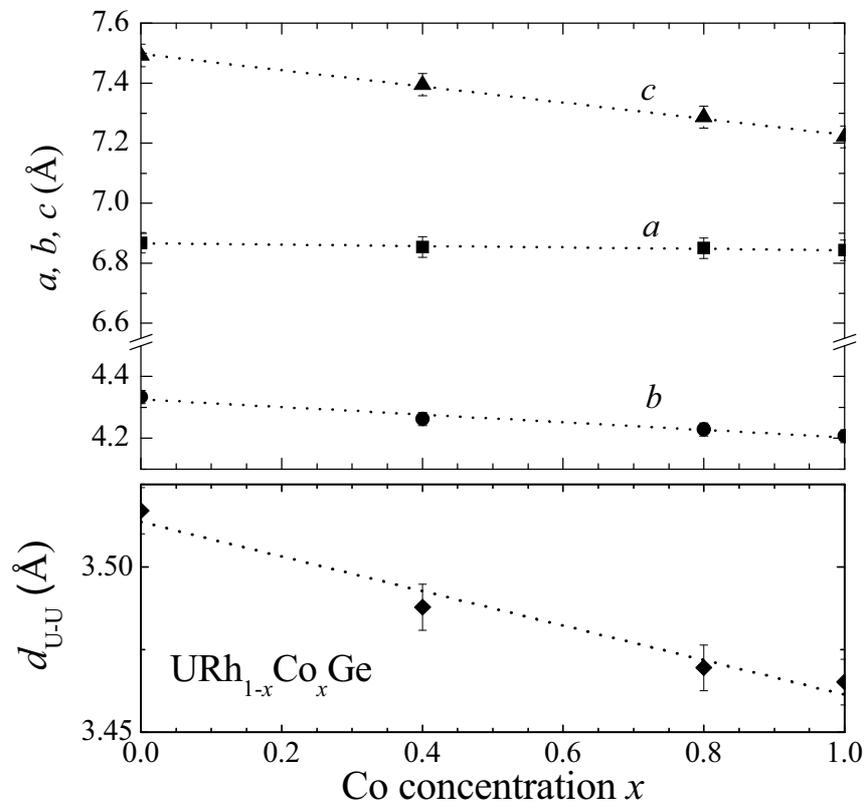
6.3.2. Magnetization

Figure 6.6 Upper frame: Lattice parameters of $URh_{1-x}Co_xGe$ as a function of Co concentration x measured at room temperature. *Lower frame*: The shortest Uranium-Uranium distance of $URh_{1-x}Co_xGe$ as a function of the Co concentration x.

The temperature variation of the magnetization $M(T)$ measured in a field of 0.01 T and its derivative d$M(T)$/dT for the URh$_{1-x}$Co$_x$Ge series are shown in Fig. 6.7. The effect of Co doping differs from that by Ru or Si doping. T_C increases monotonically up to $x = 0.6$, where it reaches a value of 20 K, *i.e.* more than twice the value for $x = 0$. For higher values of x, T_C decreases and drops to 3.0 K for the end compound UCoGe. Using the 3D Ising-like model (Eq. 4.1) to describe the $M(T)$ curves for $x \leq 0.9$ with $\alpha = 2$, we obtain for the critical exponent β values in between 0.27 - 0.37. The variation of T_C with Co concentration has also been tracked with help of Arrott plots. The Arrott plots for $x = 0.6$, where ferromagnetic order is most robust and $x = 1$, where ferromagnetic order is the weakest, are shown in Fig. 6.8.
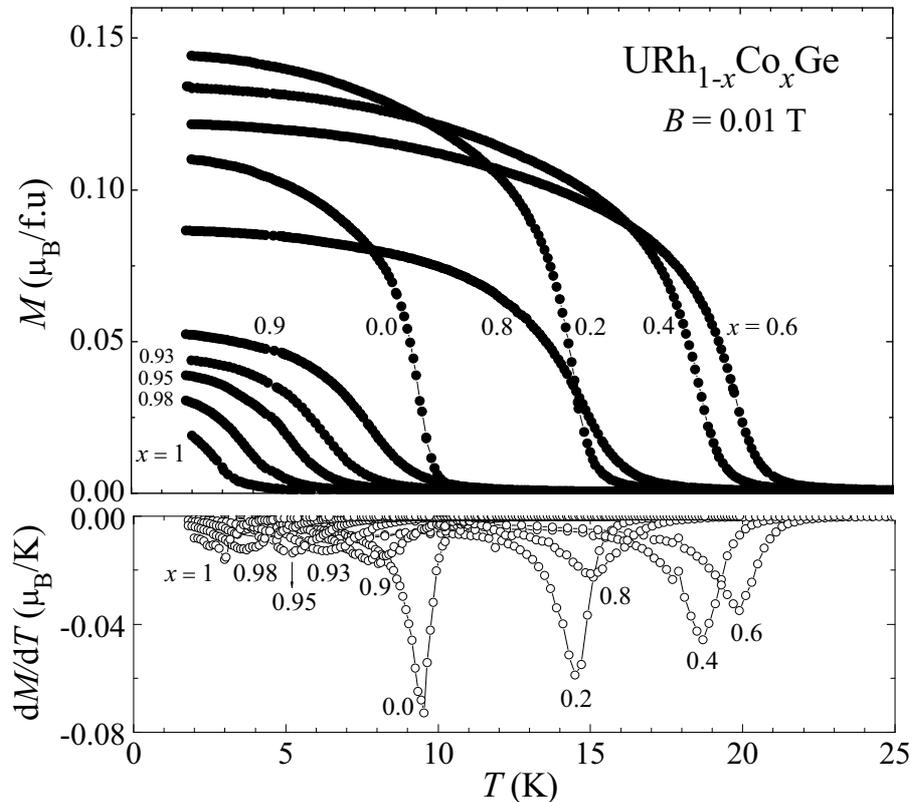

Figure 6.7 Upper frame: Temperature variation of the dc magnetization measured in a field $B = 0.01$ T of URh$_{1-x}$Co$_x$Ge alloys. Notice T_C has a maximum value for $x = 0.6$ and ferromagnetic order is observed for UCoGe with $T_C = 3$ K. *Lower frame*: Temperature derivative of the magnetization.

The discovery of ferromagnetic order below 3 K in UCoGe is surprising. In literature UCoGe was reported to be paramagnetic (at least for $T \geq 1.2$ K) [39,115]. However, the proximity to a ferromagnetic instability was conjectured on the basis of a relatively large field-induced magnetic moment of 0.58 μ_B measured in a field of 35 T [116], as well as by

a weak upturn in the specific heat, which was suppressed by a magnetic field of 5 T [154].
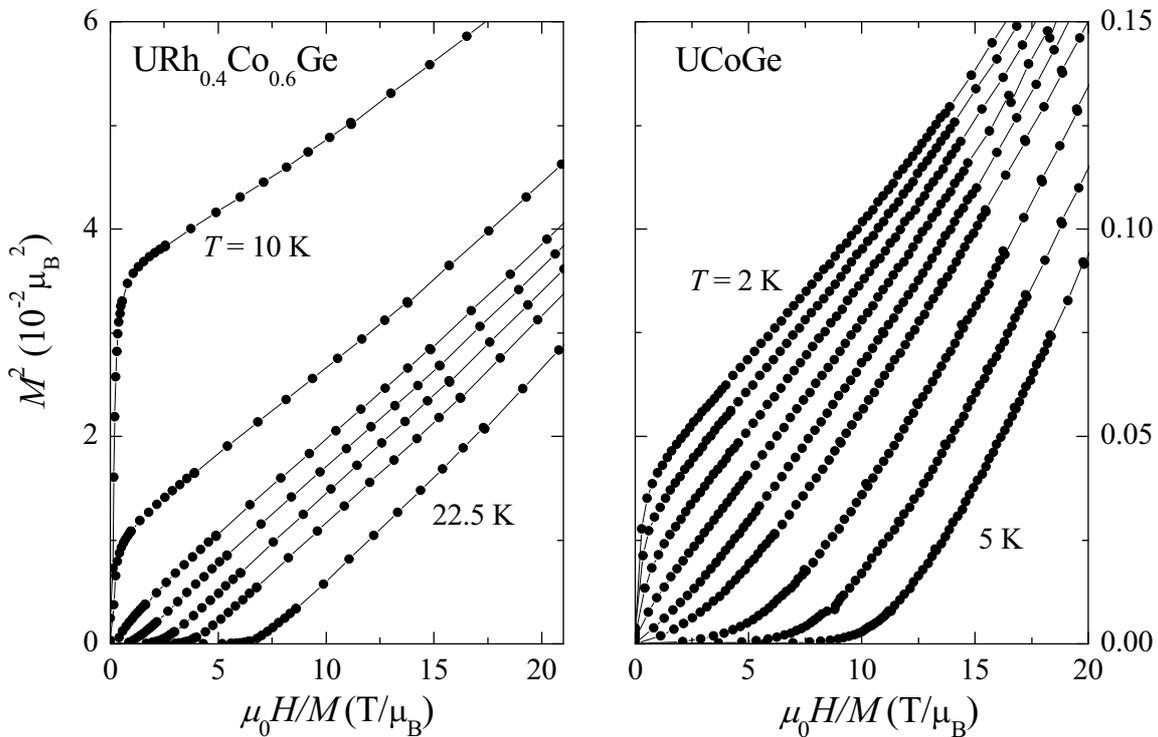

Figure 6.8 Arrott plots of the magnetization of (*left panel*) URh$_{0.4}$Co$_{0.6}$Ge with the isotherms measured (from top to down) at T = 10.0, 18.5, 20.0, 20.5, 21.0, 21.5 and 22.5 K and (*right panel*) UCoGe with the isotherms measured (from top to down) at T = 2.0, 2.3, 2.6, 2.9, 3.2, 3.5, 4.0, 4.5 and 5.0 K. The isotherm through the origin determines T_C = 20.0 and 3.0 K for URh$_{0.4}$Co$_{0.6}$Ge and UCoGe, respectively.

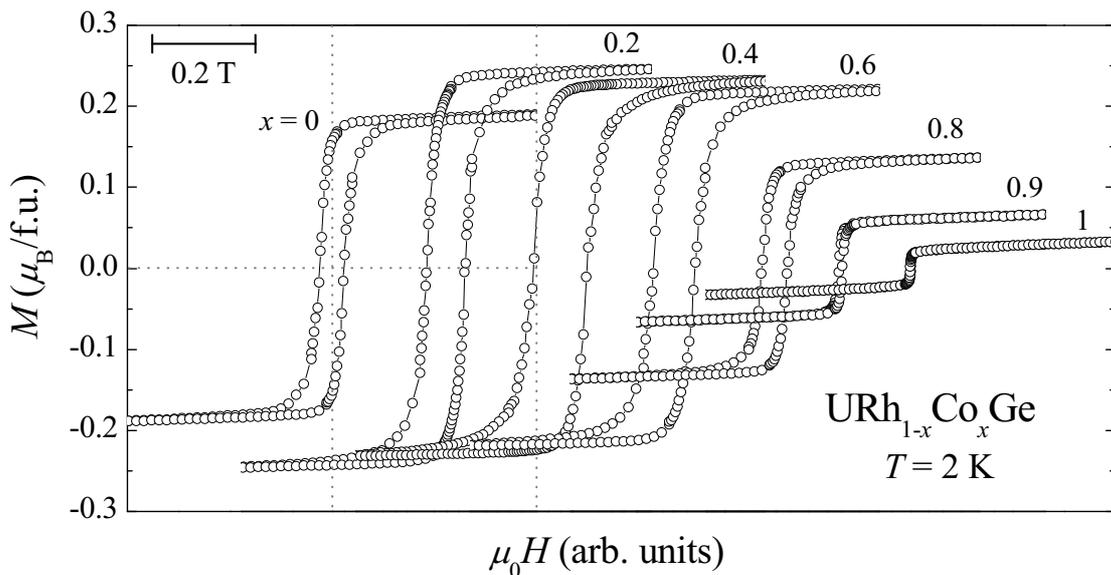*Figure 6.9* Hysteresis loops of URh$_{1-x}$Co$_x$Ge alloys measured at T = 2 K. The curves are shifted horizontally for sake of clarity. The bar gives the absolute B scale (0.2 T). Co concentrations are (from left to right) x = 0, 0.2, 0.4, 0.6, 0.8, 0.9 and 1.0.

Hysteresis loops of URh$_{1-x}$Co$_x$Ge alloys, with x in the range $0 \leq x \leq 1$, measured at $T = 2$ K in the magnetic field range -0.4 T $\leq B \leq$ 0.4 T are shown in Fig. 6.9. Notice that the curves are shifted horizontally for sake of clarity. For all samples, the loops have an *S*-shape and exhibit visible remnant moments and coercive fields. This further corroborates evidence for ferromagnetism in the entire URh$_{1-x}$Co$_x$Ge series.
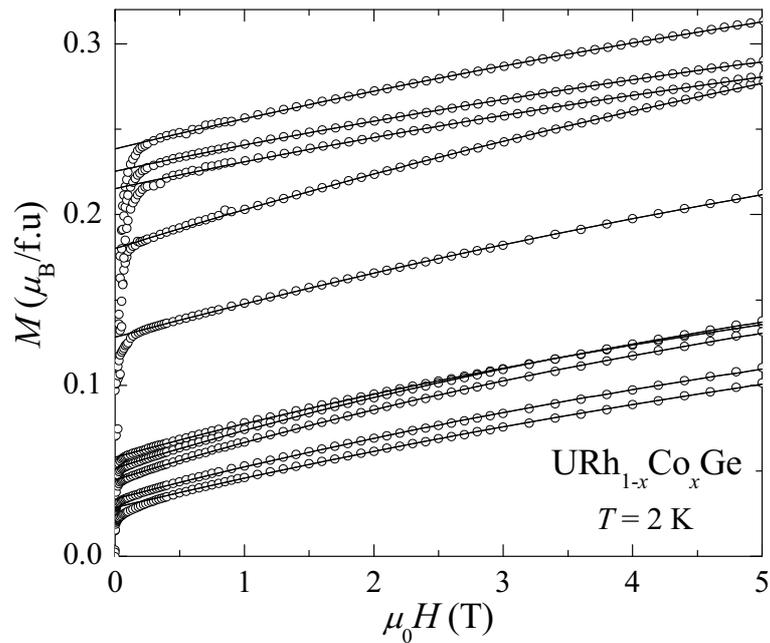

Figure 6.10 Field dependence of magnetization of URh$_{1-x}$Co$_x$Ge alloys measured in a field up to 5 T at 2 K. The lines represent fits to Eq. 4.3. Co concentrations are (from top to bottom) x = 0.2, 0.4, 0.6, 0.0, 0.8, 0.9, 0.93, 0.95, 0.98 and 1.0.
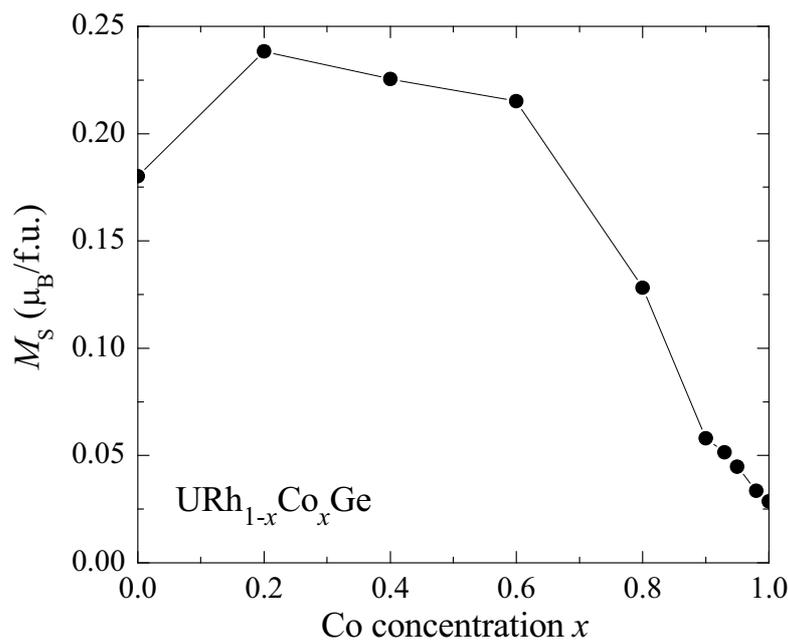

Figure 6.11 The spontaneous moment M_S of URh$_{1-x}$Co$_x$Ge as a function of Co concentration.
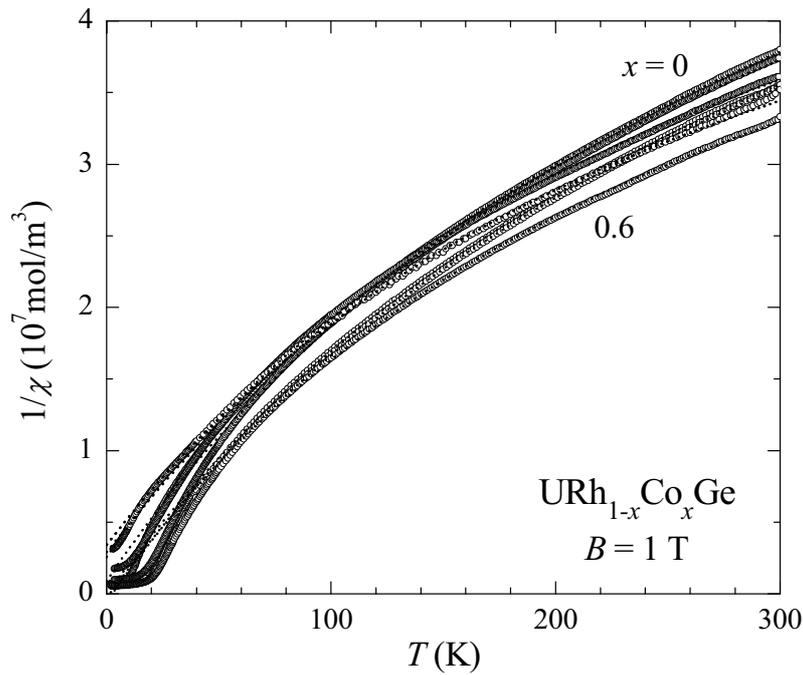
Figure 6.12 Temperature variation of the reciprocal susceptibility of $URh_{1-x}Co_xGe$ alloys with $0 \leq x \leq 1$ measured in a field of 1 T. The dotted lines are best fits to the MCW law in the temperature range 50 - 300 K. The curves show a large overlap.

Table 6.3 The Curie temperature T_C and the parameters M_S, p_{eff} and θ of $URh_{1-x}Co_xGe$ alloys deduced from the magnetization data.

x-Co	T_C (K)	M_S (μ_B/f.u.)	p_{eff} (μ_B/f.u.)	θ (K)
0	9.6	0.180	1.72	-14.1
0.2	14.5	0.238	1.72	1.0
0.4	18.7	0.225	1.73	1.6
0.6	19.9	0.215	1.69	2.5
0.8	15.0	0.128	1.64	-3.8
0.9	8.2	0.058	1.63	-11.1
0.93	6.7	0.052	1.63	-9.7
0.95	5.5	0.045	1.59	-11.4
0.98	4.1	0.034	1.61	-12.7
1	3.0	0.028	1.67	-15.7

In Fig. 6.11, we show the variation of the spontaneous magnetic moment M_S of the $URh_{1-x}Co_xGe$ series as a function of Co concentration. Here M_S is extracted from the extrapolation from higher fields towards zero field by fitting the $M(H)$ data to Eq. 4.3 (see Fig 6.10). After approaching a maximum near $x = 0.2$, M_S continuously reduces to a small

value of 0.03 μ_B/f.u. for the end compound UCoGe.

The reciprocal susceptibility of URh$_{1-x}$Co$_x$Ge measured in a field $B = 1$ T in the temperature range 2 - 300 K is shown in Fig. 6.12. The curves for various Co concentrations are very similar and have a large overlap at high temperatures. The magnetic susceptibility above 50 K follows a MCW law with $\chi_0 \sim 10^{-8}$ m^3/mol. The values of the effective moment p_{eff} and the paramagnetic Curie temperature θ are listed in Table 6.3. The ratio p_{eff}/M_S is much large than 1 which confirms the delocalization of 5f states in URh$_{1-x}$Co$_x$Ge [82,132].

6.3.3. Electrical resistivity

The temperature dependence of the electrical resistivity $\rho(T)$ of the URh$_{1-x}$Co$_x$Ge alloys is presented in Fig. 6.13. Note that the vertical scale is in arbitrary units and the curves are shifted for clarity. For $x \leq 0.6$ the resistivity data show a weak maximum near 100 K (see the left panel of Fig. 6.13) followed by a rapid drop when ferromagnetism sets in. For $x \geq 0.8$ coherence effects appear before the transition to the FM state.

Table 6.4 The Curie temperature T_C and the parameters ρ_0, n and A obtained by fitting the resistivity to $\rho = \rho_0 + AT^n$ for URh$_{1-x}$Co$_x$Ge alloys.

x-Co	T_C (K)	T_S (K)	ρ_0 ($\mu\Omega$cm)	n	A ($\mu\Omega$cm/K^2)
0	9.4	-	78	2	6.21
0.2	14.6	-	228	2	1.62
0.4	18.5	-	294	2	1.10
0.6	19.7	-	304	2	0.96
0.8	14.5	-	235	2	2.07
0.9	7.6	-	232	2	2.45
0.93	6.4	-	198	2	3.80
0.95	5.4	-	157	2	4.03
0.98	3.9	0.41	108	2	7.28
1	2.8	0.46	84	2	6.92

The resistivity at low temperatures ($T < 25$ K) is shown in the right panel of Fig. 6.13. The magnetic phase transition at T_C shows up as a kink in $\rho(T)$, which broadens with increasing Co concentration. The Curie temperatures, which are determined by the maximum in dρ/dT (arrows in Fig. 6.13), are in good agreement with values obtained by the magnetization

measurements. For all samples, the resistivity drops steadily below T_C where it follows the relation $\rho = \rho_0 + AT^n$ (Eq. 4.5) with exponent $n = 2 \pm 0.15$, signaling scattering at magnons.

For the end compound UCoGe, superconductivity is observed below 0.5 K (for a sample with residual resistance ratio $RRR \sim 10$). The critical temperature, T_S, is taken by the midpoints of the transition and equals to 0.46 K. In the samples with lower Co concentration ($x \leq 0.95$), the SC state is strongly influenced by disorder. T_S is reduced to 0.41 K for $URh_{0.02}Co_{0.98}Ge$ and no sign of SC is detected in the resistivity measurement down to 50 mK for $x = 0.95$ ($RRR \approx 6$). In Table 6.2 we summarize the relevant parameters extracted from the resistivity measurements.
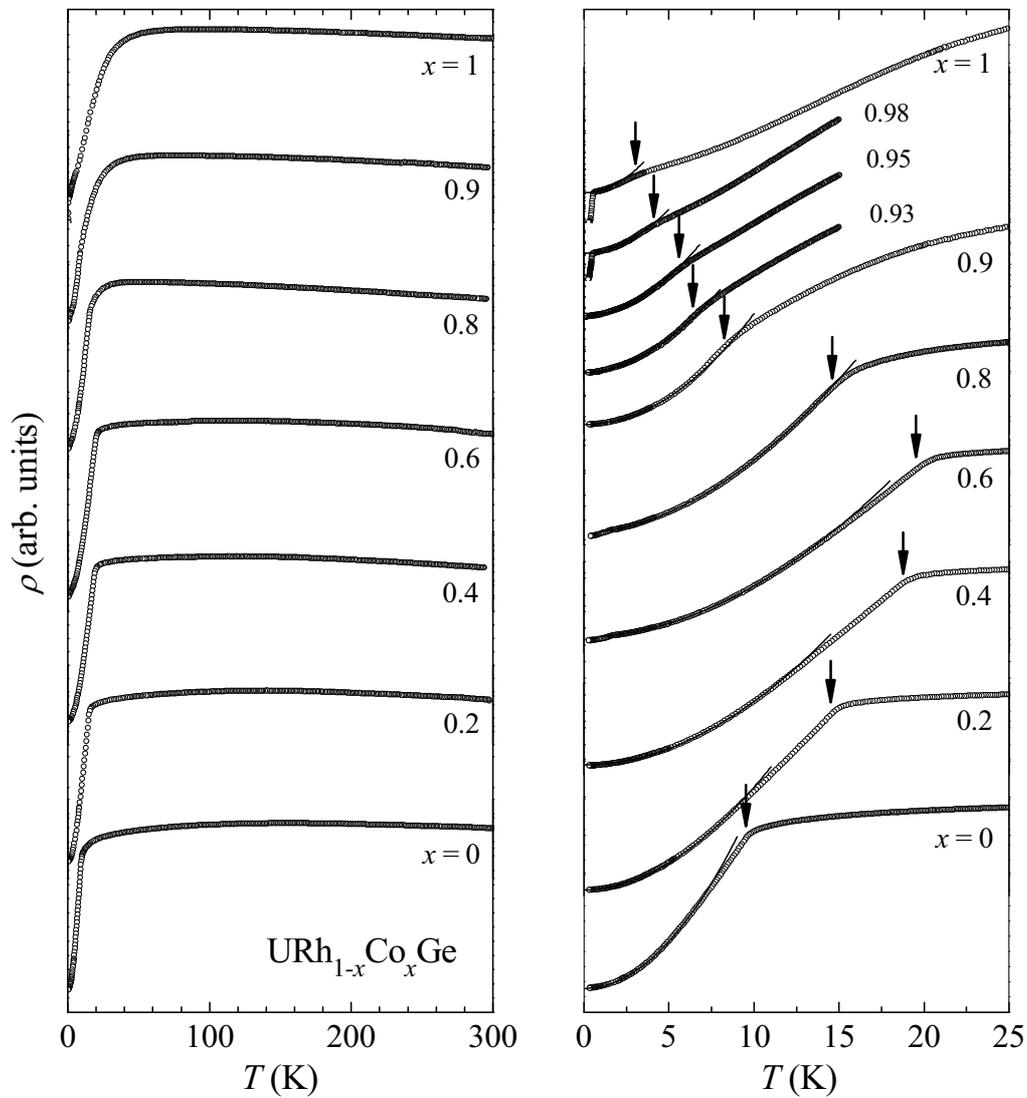

Figure 6.13 Temperature dependence of the electrical resistivity ρ in arbitrary units of $URh_{1-x}Co_xGe$ alloys for $0 \leq x \leq 1$ as indicated. *Left panel*: 2 K $\leq T \leq$ 300 K. *Right panel*: 0.25 K $\leq T \leq$ 25 K. The Curie temperatures are indicated by arrows. The solid lines represent fits to $\rho = \rho_0 + AT^n$.
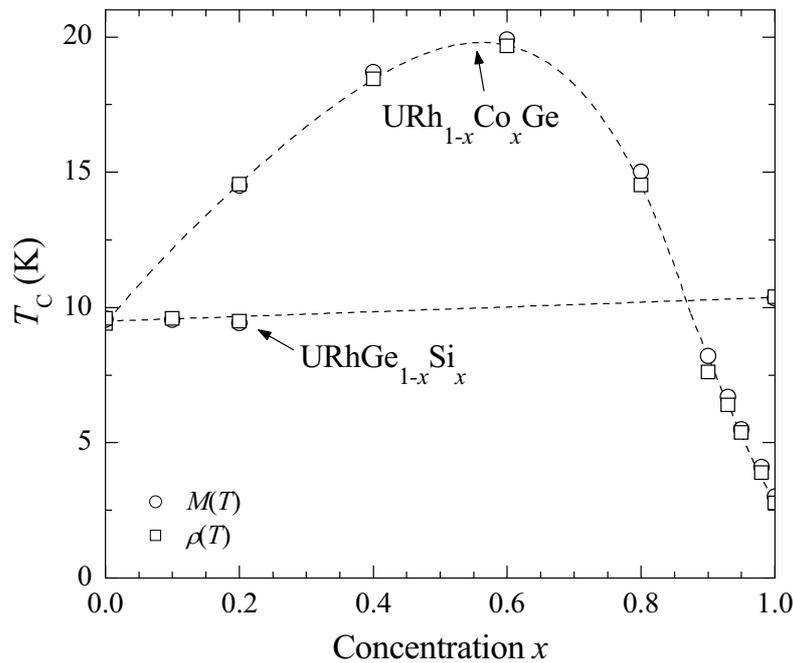
6.4. Discussion

Figure 6.14 The Curie temperature of URhGe$_{1-x}$Si$_x$ and URh$_{1-x}$Co$_x$Ge alloys as a function of Si and Co concentration determined from $M(T)$ and $\rho(T)$. The line serves to guide the eye.

The magnetic phase diagram $T_C(x)$ of URhGe doped with Si and Co is presented in Fig. 6.14. Here the Curie temperatures are determined from the magnetization and resistivity data. Doping up to 20 at.% Si on the Ge site does not suppress ferromagnetic order and T_C remains 9.5 K, while for the end compound URhSi T_C = 10.4 K. We conclude that the ferromagnetism does not significantly change in the entire URhGe$_{1-x}$Si$_x$ series. The $T_C(x)$ curve for Co substitution follows a Doniach-like diagram: T_C first increases up to 20 K for x = 0.60, beyond which it reduces to 3 K for x = 1.0. This is similar to the variation of $T_C(x)$ in the case of URh$_{1-x}$Ru$_x$Ge. However, in a quantitative measure Co is less than half as effective as Ru in suppressing T_C. Interestingly, the end compound UCoGe is a ferromagnetic superconductor, just like URhGe.

In order to compare the volume effects due to alloying and hydrostatic pressure, we use an isothermal compressibility $\kappa = -V^{-1}(\mathrm{d}V/\mathrm{d}p)$ = 0.8 Mbar^{-1}, and calculate from the lattice parameter variation that substitution of 1 at.% Co and Si leads to a chemical pressure of 0.91 kbar and 0.46 kbar, respectively. With $\mathrm{d}T_C/\mathrm{d}p$ = 0.065 K/kbar as derived from the resistivity measurements under pressure [120] we calculate an increase of T_C per at.% Co and Si of 0.059 and 0.030 K, respectively. In the case of Co doping the calculated value is

about a factor 5 too small when compared to the measured initial increase in T_C (see Fig. 6.14), while in the case of Si doping T_C does not increase at all. This shows that just like in the case of Ru doping (see Chapter 4) chemical and mechanical pressure are not equivalent.

The evolution of magnetism in the $URh_{1-x}Co_xGe$ alloys follows a Doniach-like phase diagram [28,142,143]. However, the variation of $T_C(x)$ cannot be understood in a simple way. Anisotropic hybridization phenomena related to the anisotropic variation of the unit cell parameters make a direct comparison between the effect of Ru, Si or Co doping in URhGe difficult. Moreover, Si and Co are iso-electronic substitutions, while Ru is not. Specific-heat measurements would be helpful to further elucidate the hybridization phenomena and the evolution of magnetism in the $URh_{1-x}Co_xGe$ series.

In summary, our search for the magnetic instability of URhGe by chemical substitution of Ru (see Chapter 4) and Co has led to the discovery of two unique materials:

(i)   In the $URh_{1-x}Ru_xGe$ series a FM QCP is found near $x_{cr} = 0.38$. This is the first *f*-electron system exhibiting a FM QCP at ambient pressure.

(ii) The end compound of the $URh_{1-x}Co_xGe$ series, UCoGe, is a new member of the family of ferromagnetic superconductors. Ferromagnetic order with a low Curie temperature $T_C = 3$ K and a small ordered moment $m_0 = 0.03$ μ_B coexists with superconductivity below 1 K. This indicates UCoGe is close to the ferromagnetic instability. A detailed investigation of the superconducting and magnetic properties of UCoGe is presented in Chapter 7.